AUT Journal of Mechanical Engineering

AUT J. Mech. Eng., 7(2) (2023) 175-184
DOI: 10.22060/ajme.2023.21808.6046

Perforation study of steel sheet under high velocity impact using Peridynamic theory

Sayyed Roohollah Kazemi[1]*, Meisam Shakouri[2]

[1] Faculty of Mechanical Engineering, University of Guilan, Guilan, Iran.
[2] Faculty of New Sciences and Technologies, Semnan University, Semnan, Iran.

ABSTRACT: Peridynamic theory is a new method to model material behavior under impact loading. The simplest type of this method is called bond-based peridynamics. The present study is concerned with the modification of the bond-based peridynamic theory to account for inelastic behavior and the modified theory is used to study the dynamic fracture of plates, made of ductile materials, due to impact. This theory assumes that the bonds between two points can bear stretches more than the yield stretch. In this regard, The modified bond-based theory is used to study the effect of penetration, resulting from the impact of a projectile into a rectangular steel sheet. The results are validated against experimental results, and the crack growth and its propagation paths are studied for different geometric shapes and impact velocities of the projectiles. The results show that with this modification, the bond-based peridynamics could be employed more inclusively to simulate the behavior of materials.

Review History:

Received: Oct. 02, 2022
Revised: May, 13, 2023
Accepted: Sep. 02, 2023
Available Online: Sep. 12, 2023

Keywords:

Peridynamic Theory
Modified bond-based
Perforation
Steel sheet

1- Introduction

The failure of structures due to the impact, known as dynamic fracture, is one of the fundamental problems in fracture science [1] and many studies have been done with different methods on this phenomenon [2-5]. The failure of the structures by increasing static load is entirely different from the dynamic fracture because the propagations of the stress wave -which is the main source of dynamic fracture- varies with material properties and geometrical configuration of the structure. As a result, the modeling and simulation of the impact damage to predict the crack initiation, growth, and branching has attracted great attention.

One of the main problems in the simulation of the crack initiation and growth in the materials returns to the mathematical flaws that arise in the framework of classical continuum mechanics. The problem is that because of the discontinuities resulting from the material damage and failure, the mathematical formulation, which is a set of partial differential equations, cannot be applied to the impact region. Therefore, the continuum-based formulation needs additional models, like the cohesive zone model (CZM) [6] and extended finite element model (XFEM)[7, 8], for discontinuities.

In recent years, the peridynamic theory has been introduced to overcome the flaws of the continuum methods in the modeling of the initiation and growth of cracks [9, 10]. The difference between the peridynamic theory and the classical theory, as well as most nonlocal theories, is that it does not involve spatial derivatives of the displacement field. Instead, it is formulated in terms of integral equations, whose validity is not affected by the presence of discontinuities such as cracks. It may be thought of as a “continuum version of molecular dynamics” in which each particle interacts with the particles located in its neighborhood [11, 12].

Because of the benefits of considering discontinuities within a single continuum framework, the peridynamic theory is being employed in increasing applications in impact analyses. Silling and Askari [12] employed the peridynamic modeling for impact damage in brittle materials including simulations of a Charpy V-notch test, accumulated damage in concrete due to multiple impacts, and crack fragmentation of a glass plate. Xu et al. [13] employed peridynamic theory to study the impact damage in composite laminates and compared the results with experimental data. Kazemi [14] investigated the ductile behavior of a steel strip induced by the high-velocity impact of various projectile shapes using the ordinary state-based peridynamic method Bobaru et al. [15] simulated the damage progression from impact with a high-velocity projectile in a layered glass by using peridynamics. They showed that many of the damage morphologies reported in the experiments are captured by the peridynamic results. Oterkus et al. [16] applied peridynamic theory for predicting the residual strength of impact-damaged reinforced panels,

---

*Corresponding author’s email: kazemi@guilan.ac.ir

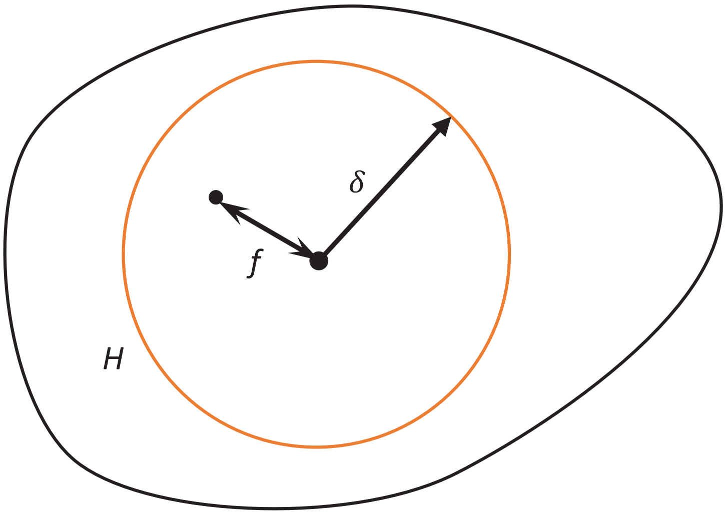

Fig. 1. Interaction of material point with its neighboring points

and validated their results against experiment results of fracture of concrete. Liu et al. [17] studied the impact damage in a three-point bending beam with an offset notch which is used to investigate the mixed I-II crack propagation in brittle materials. Chen et al. [18] applied the bond-based peridynamic theory in predicting beam vibration and impact damage made of brittle materials. Lee et al. [19] implemented a new contact algorithm to capture the interaction of peridynamics and finite element method for impact fracture analysis.

Silling et al. [20] studied the impact phenomena with the Eulerian representation of peridynamics, in which bond forces depended only on the positions of material points in the deformed configuration. Sun and Huang [21] applied peridynamic simulation to impacting damage in composite laminate and Zhang et al. [22] analyzed shear damage propagation and crack growth from edge-on impact. Song et al. [23] employed non-ordinary state-based peridynamics to study ice fragmentation by impact, and Baber et al. [24]investigated the low-velocity impact damage in laminated composites reinforced with z-pins using peridynamic theory. Zhou and Liu [25] analyzed the intralayer damage and delamination in laminated composite plates induced by impact.

Zheng et al. [26] employed peridynamics to simulate the failure of reinforced concrete T-beam under impact loading and Wu and Huang [27] implemented a Hertz-peridynamic model to analyze energy dissipation from normal elastic impact at low and high impact velocities. Jafaraghaei et al. [28] used bond-based peridynamics and studied the dynamic failure process of glass plates subjected to high-velocity impact loads and Sun et al. [29] proposed a bond-based peridynamics with the introduction of plastic hardening of the resin matrix for fiber-reinforced polymer composites to analyze the impact damage of composite materials.

By reviewing the literature, it seems that many of the investigations with the bond-based peridynamic method have been focused on brittle fracture, and ductile materials have been less investigated. The main idea of the present paper is to implement a modification on the bond-based peridynamic theory, proposed by [30], to account for the inelastic behavior of materials and to employ the modified bond-based theory to study the dynamic fracture of plates, made of ductile materials, due to impact.

2- Peridynamic Model for Elastic-Plastic Impact Analysis

2- 1- Bond-Based Peridynamic Theory

According to the peridynamic theory, the motion of the body is analyzed by considering the interaction of a particle, **x**, with the other particles in the body. The influence of the material points interacting with **x** is assumed to exist in the neighborhood of the region (horizon), denoted by H as shown in Fig. 1. The state of any material point is determined by its pairwise interaction with the points located within a finite distance, called the horizon, which is represented by δ.

In bond-based peridynamic theory, the force vectors between the pair **x** and $\mathbf{x}'$ and vise-versa are equal in magnitude and parallel to the relative position vector in the deformed state, to satisfy the requirement for the balance of angular momentum [10] and the equation of the motion of the material point **x** is [31]:

$$\rho(\mathbf{x})\ddot{\mathbf{u}}(\mathbf{x},t)=\int_{H}\mathbf{f}(\mathbf{u}-\mathbf{u}',\mathbf{x}-\mathbf{x}',t)dH+\mathbf{b}(\mathbf{x},t) \tag{1}$$

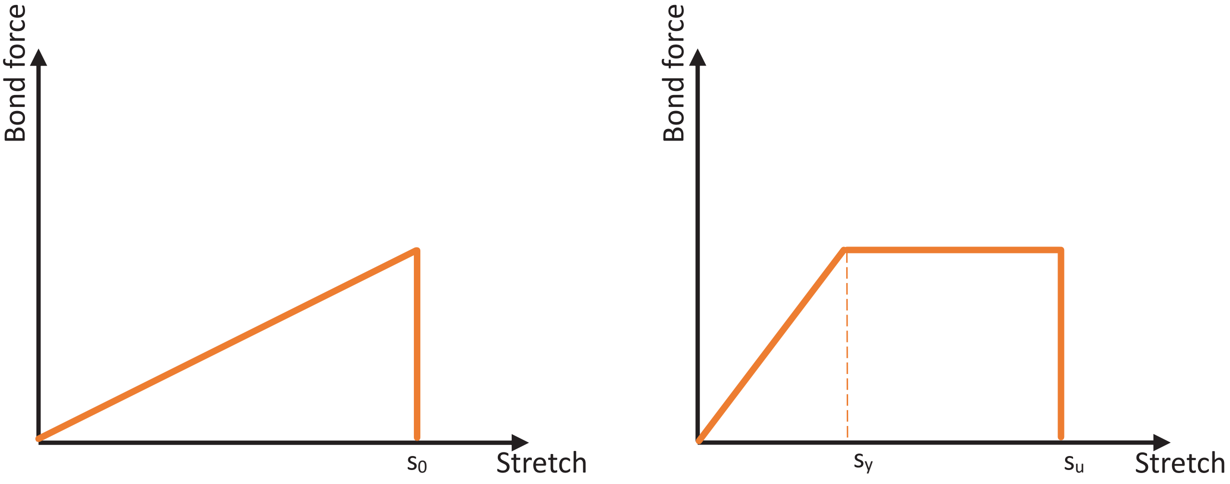

(a) (b)

Fig. 2. (a) Bond force as a function of bond stretch in a brittle material model; (b) bond force as a function of bond stretch in a ductile material model [30].

in which ρ is the mass density, $\mathbf{b}$ is the body force vector, $\mathbf{u}$ and $\mathbf{u}'$ is the displacement vectors of the material points $\mathbf{x}$ and $\mathbf{x}'$, respectively, and $\mathbf{f}$ is the force density vector acting on the particle $\mathbf{x}$ from $\mathbf{x}'$ in its horizon. The pairwise force function is [17]:

$$\mathbf{f}(\boldsymbol{\eta},\boldsymbol{\xi}) = c(\boldsymbol{\xi}) s(\boldsymbol{\eta},\boldsymbol{\xi}) \frac{\boldsymbol{\eta}+\boldsymbol{\xi}}{|\boldsymbol{\eta}+\boldsymbol{\xi}|} \qquad (2)$$

where $\mathbf{î} = \mathbf{x}' - \mathbf{x}$ is the relative position, and $\mathbf{ç} = \mathbf{u}' - \mathbf{u}$ is the relative displacement vector in the reference configuration, $c(\mathbf{î})$ is the material property in peridynamics, and $s(\mathbf{ç},\mathbf{î})$ is the bond stretch (the relative elongation).

2- 2- Modified bond-based peridynamics including plastic effects

In classical Bond-Based Peridynamics, when the bond stretch between two material points, i.e., $\mathbf{x}'$ and $\mathbf{x}$, reaches a critical stretch value s_0, failure occurs suddenly and the interaction between these two points is removed. (see Fig. 2(a)). This critical stretch s_0 is obtained by equating the work per unit fractured area, for which all the bonds across a surface to the fracture energy G_0 should be broken and completely separated along the surface.

To account for the plastic behavior, the modified bond-based peridynamics assumes that the bonds between two points can bear stretches more than critical stretches. Fig. 2(b) modifies the bond-based peridynamic theory to account for the plastic behavior of ductile material. According to this model, the bond yields at the yield limit s_y, and continues the stretch up to the ultimate stretch s_u [30].

2- 3- Numerical Solution Method

Since the governing equations are integral-form in space and differential-form in time, first a numerical technique is utilized for spatial integration. For this purpose, the meshless collocation scheme is performed (as seen in Fig. 3(a)) and the domain is divided into a finite number of material points with particular volumes which act as integration points. Since the volume of the material points located near the boundaries of each horizon is not entirely set in the horizon, a correction factor is used to modify the volume involvement. The numerical time integration is implemented by utilizing explicit integration schemes, which have been described in Ref. [31] in detail and is not repeated in this paper for the sake of brevity.

2- 4- Impact Modeling

In this paper, the projectiles are molded as a rigid body with the initial velocity of v_0, as illustrated in Fig. 3(a). The deformable target material points follow the peridynamic equations of motion (see Eq. (1)). After the initial indentation of the projectile into the target, which is shown in Fig. 3(b), the material points that are placed inside the impactor are moved to their new locations outside the impactor that is closest to the surface of it, as shown in Fig. 3(c). Therefore, according to the energy of the impactor, the penetration procedure at any time, t, can be modeled with this progressive procedure [31].

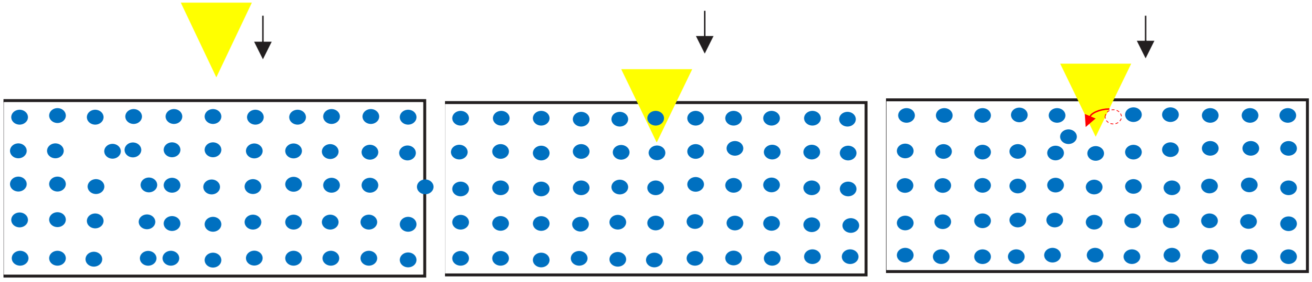
(a) t (b) $t+\Delta t$ (c) $t+\Delta t$

Fig. 3. Movement of material points inside a target material induced by impact

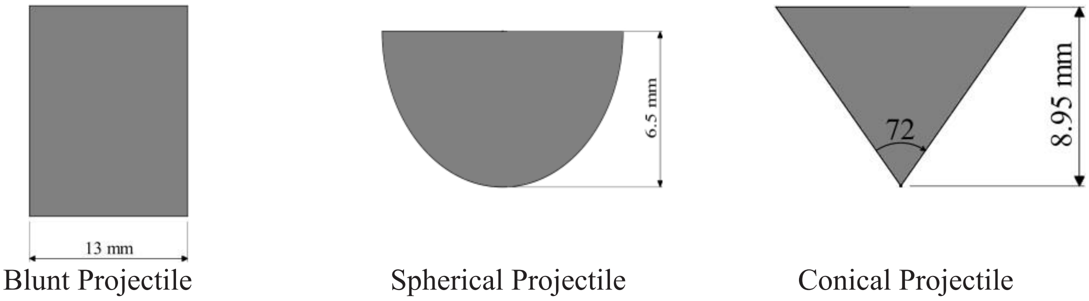

Fig. 4. Geometry of projectiles [32]

The velocity of such a material point, $\mathbf{x}_i$, in its new position at the next time step, $t+\Delta t$, can be calculated from

$$\bar{\mathbf{v}}_i^{t+\Delta t} = \frac{\bar{\mathbf{u}}_i^{t+\Delta t} - \mathbf{u}_i^{t}}{\Delta t} \tag{3}$$

where $\bar{\mathbf{u}}_i^{t+\Delta t}$ is the modified displacement vector at time $t+\Delta t$, $\mathbf{u}_i^t$ indicates the displacement vector at time t, and Δt corresponds to the time increment value. At time $t+\Delta t$, the effect of the material point, $\mathbf{x}_i$, on the reaction force from the target material to the impactor, $\mathbf{F}_i^{t+\Delta t}$, can be calculated as

$$\mathbf{F}_i^{t+\Delta t} = -1\times\rho_i \frac{\bar{\mathbf{v}}_i^{t+\Delta t} - \mathbf{v}_i^{t+\Delta t}}{\Delta t} V_i \tag{4}$$

where $\mathbf{v}_i^{t+\Delta t}$ is the velocity vector at time $t+\Delta t$ before relocating the material point $\mathbf{x}_i$, with ρ_i and V_i denoting its density and volume, respectively. Summation of the contributions of all material points inside the impactor results in the total reaction force, $\mathbf{F}^{t+\Delta t}$, on the impactor at time $t+\Delta t$ [31].

3- Peridynamic results for impact damage in steel plate using modified BBPD

3- 1- Problem Setup

In this study, the effect of impact and penetration phenomena resulting from the impact of projectiles with different geometric shapes and at different speeds into a rectangular steel sheet has been investigated. Three spherical, blunt, and conical shapes are selected for projectiles and the impact velocity range is approximately 70 to 180 m/s. The projectiles have a mass of about 30 grams and their dimensions are the same as [32], a view of them is given in Fig. 4.

The geometric and mechanical properties of the target sheet are also similar to [30] and are presented in Table 1 and Fig. 5. In Table 1, K_{Ic} is referred to critical stress intensity factor and also the s_y is set to 0.006 and the s_u is 0.03.

3- 2- Comparative study

To ensure that the plastic behavior is captured by the modified BBPD model, the results of the present numerical analysis were compared with a perforation test on ductile steel with significant plastic effects. The comparison between present numerical results and experimental results done by Kpenyigba et al. [32] for the projectiles with spherical, conical,

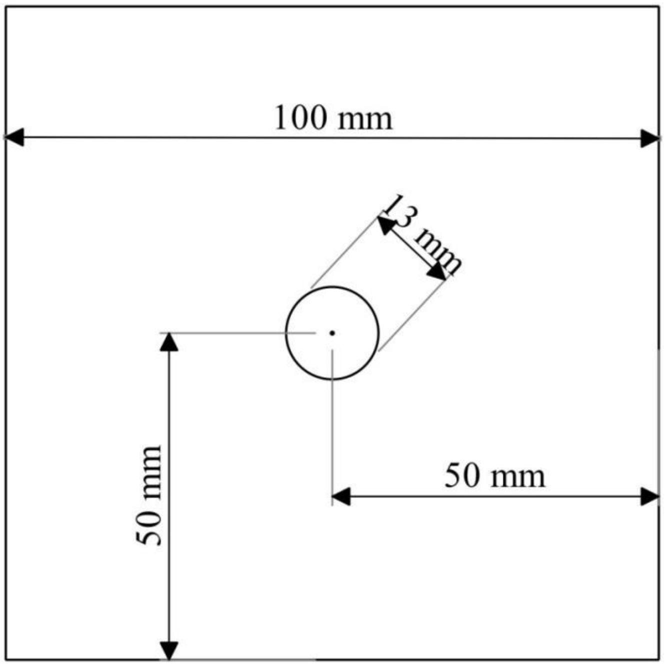

Fig. 5. Geometry of steel plate (thickness = 1mm) [32]

Table 1. Material parameters of the plate [30]

E (GPa)	σ_Y (MPa)	ν	K_{Ic} (MPa . m$^{1/2}$)
200	154	0.25	50

and blunt tips are shown in Fig. 6 (a) – (c), respectively. Good accordance between the numerical and experimental results can be observed.

3- 3- Crack propagation paths

In Figs. 7 and 8, the starting and growth pattern of the crack in the sheet over time, due to the impact of a hemispherical projectile, is given for two initial velocities of 100 and 180 m/s. As it is shown, one can see the “edge back” phenomenon in some parts of the damage process.

3- 4- Effects of impactor shapes and velocity

In Fig**.** 9 and 10, the comparison between the trends of the post-impact velocity reduction of projectiles with different shapes is given for two initial impact speeds. As can be seen, the rate of slowdown is the highest for the blunt projectile and the lowest for the conical projectile. It is also observed that, for an impact speed of 100 m/s, the overall speed reduction for spherical heads is considerably higher than other projectiles. This means that the absorbed energy before failure is almost the same for blunt and conical projectiles and lower than hemispherical ones. This is mainly because the process of plastic strain localization for hemispherical shape projectiles occurs with a delay. For a blunt projectile, the plastic work is needed to plug out of the target due to shear. However, for a spherical nose shape, the steel sheet flows along the projectile nose to induce a circumferential necking followed by a plug ejection. This process requires more plastic work than that is necessary for the blunt nose. This is thoroughly discussed in [30, 33].

At the higher velocity impact, i.e. 180 m/s, the amounts of velocity reduction for all three projectiles are nearly equal, and in comparison with the previous case (which was closer to the ballistic limit), the absorbed energy is less dependent on the projectile shape. This is similar to the results obtained by Kpenyigba et al. [32].

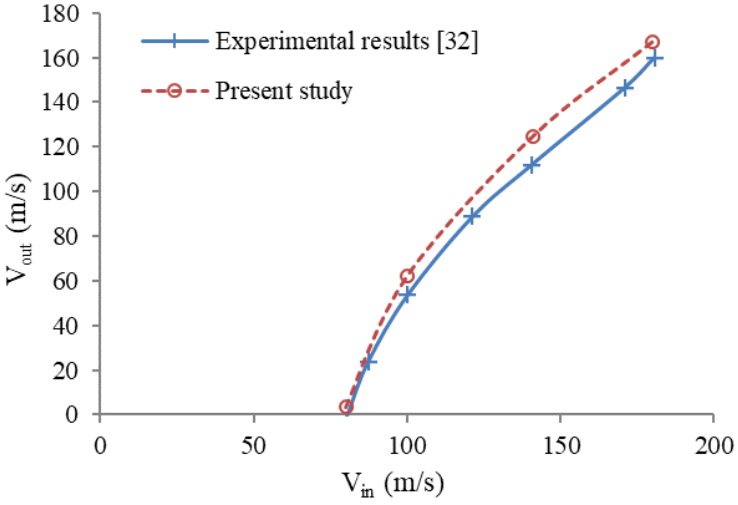

(a) Spherical

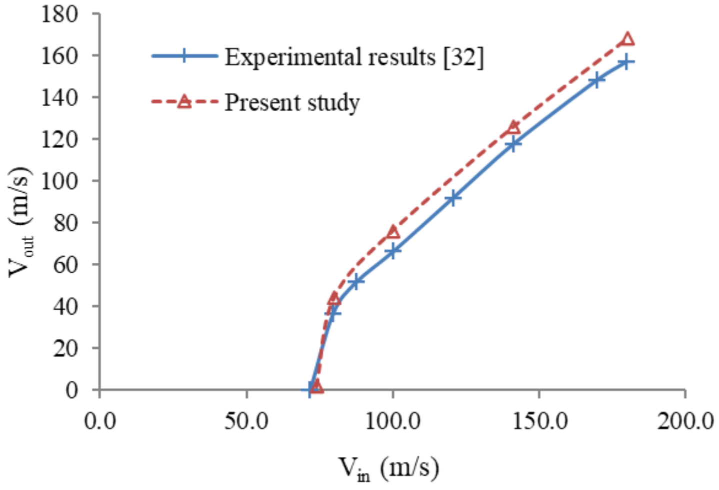

(b) Conical

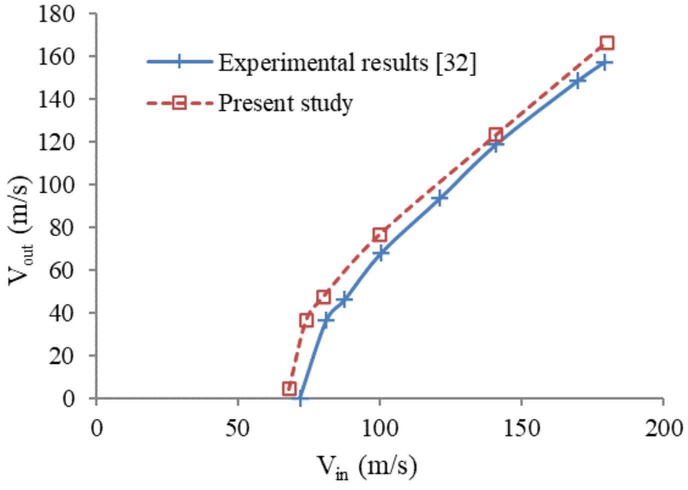

(c) Blunt

Fig. 6. Comparison of the ballistic curves obtained from present and experimental results for various projectile shapes

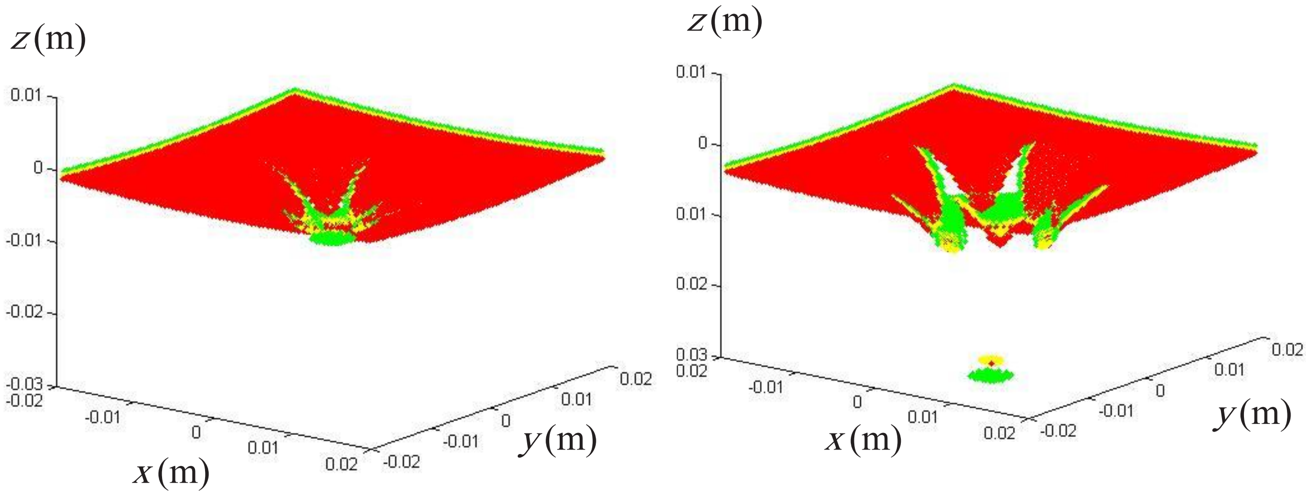

(a) t = 120 μs

(b) t = 360 μs

Fig. 7. Failure patterns for hemispherical projectile and v=100 m/s

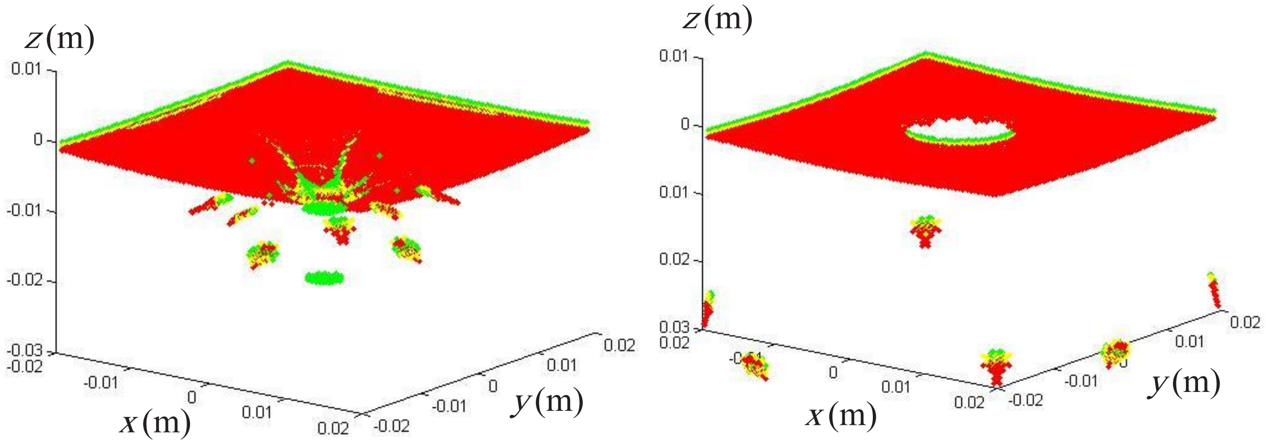

(a) t = 120 μs

(b) t = 360 μs

Fig. 8. Failure patterns for hemispherical projectile and v=180 m/s

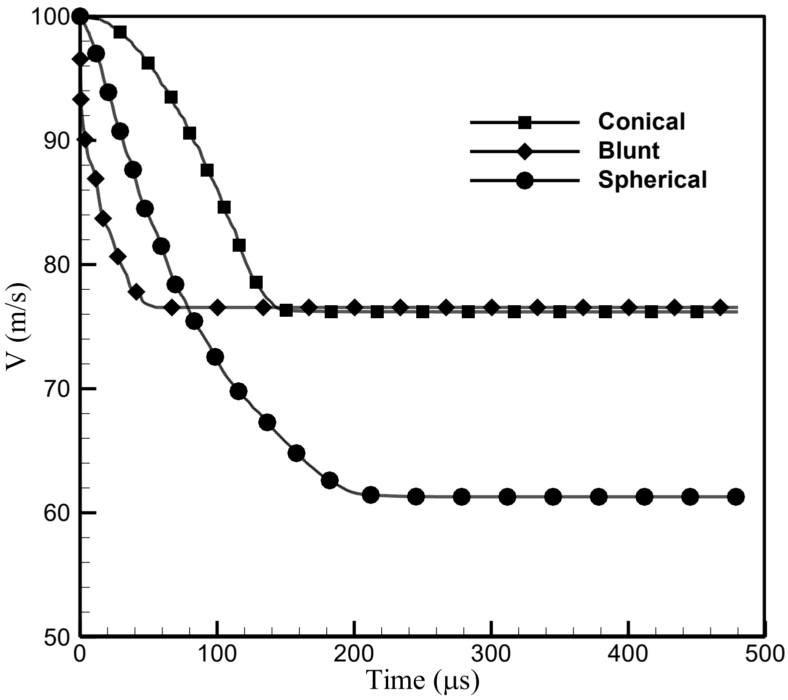

Fig. 9. Projectiles velocity (Vin=100 m/s)

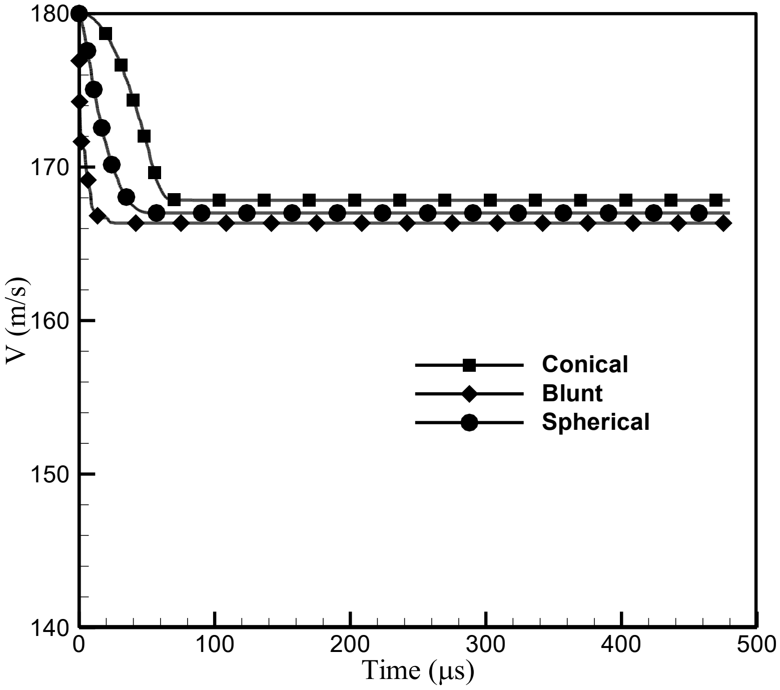

Fig. 10. Projectiles velocity (Vin=180 m/s)

4- Conclusion

In this paper, a modified bond-based peridynamic theory was employed to account for the inelastic behavior of ductile materials to study the dynamic fracture of plates due to impact. The modified bond-based peridynamics assumes that the bonds between two points can bear stretches more than the yield stretch. The modified bond-based theory was used to study the effect of penetration, resulting from the impact of projectile into a rectangular steel sheet. The results were validated against experimental results and the crack growth and its propagation paths were studied for different geometric shapes and impact velocities. As it is expected, at both impact speeds, the rate of slowdown was the highest in the case of the blunt projectile. and was the lowest for the conical projectile. It was also observed that, for an impact speed of 100 m/s, the overall speed reduction for the spherical head was considerably higher than for other projectiles. However, at the higher velocity impact, i.e. 180 m/s, the amount of velocity reduction for all three projectiles was nearly equal. The results show that with this modification, the bond-based peridynamics could be employed more inclusively to simulate the behavior of materials, and in some cases, the formation of petal-like shapes in the steel sheet could be observed at the impact position in some parts of the damage process.

Acknowledgment

This work has been supported by the High Performance Computing Research Center (HPCRC) - Akmirkabir university of Technology.

References

[1] B.N. Cox, H. Gao, D. Gross, D. Rittel, Modern topics and challenges in dynamic fracture, Journal of the Mechanics and Physics of Solids, 53(3) (2005) 565-596.

[2] S.A. Mousavizadeh, M. Hosseini, H. Hatami, Experimental Studies on Energy Absorption of Curved Steel Sheets under Impact Loading and the Effect of Pendentive on the Deformation of Samples, Journal of Modeling in Engineering, 18(63) (2021) 27-40.

[3] H. Sepahvand, M. Hosseini, H. Hatami, Experimental and Numerical Investigation on Concrete Specimens with Expanded Metal Sheet under Impact Loading, Journal of Applied and Computational Sciences in Mechanics, 32(1) (2021) 211-230.

[4] R. Azarafza, A. Davar, Analysis and Optimization of Fibre-Metal Laminate Cylindrical Shells Subjected to Transverse Impact Loads, AUT Journal of Mechanical Engineering, 4(4) (2020) 535-552.

[5] S. Sadeghnejad, Y. Taraz Jamshidi, M. Sadighi, On the Low-Velocity Impact and Quasi-Static Indentation Studies of Nomex Honeycomb Composite Sandwich Panels, AUT Journal of Mechanical Engineering, 3(2) (2019) 243-254.

[6] G.I. Barenblatt, The formation of equilibrium cracks during brittle fracture. General ideas and hypotheses. Axially-symmetric cracks, Journal of Applied Mathematics and Mechanics, 23(3) (1959) 622-636.

[7] J. Dolbow, T. Belytschko, A finite element method for crack growth without remeshing, International Journal for Numerical Methods in Engineering, 46(1) (1999) 131-150.

[8] T. Belytschko, T. Black, Elastic crack growth in finite elements with minimal remeshing, International Journal for Numerical Methods in Engineering, 45(5) (1999) 601-620.

[9] S.A. Silling, E. Askari, A meshfree method based on the peridynamic model of solid mechanics, Computers & Structures, 83(17-18) (2005) 1526-1535.

[10] S.A. Silling, Reformulation of elasticity theory for discontinuities and long-range forces, Journal of the Mechanics and Physics of Solids, 48(1) (2000) 175-209.

[11] P. Seleson, M.L. Parks, M. Gunzburger, R.B. Lehoucq, Peridynamics as an upscaling of molecular dynamics, Multiscale Modeling & Simulation, 8(1) (2009) 204-227.

[12] S.A. Silling, E. Askari, Peridynamic modeling of impact damage, in: ASME/JSME 2004 Pressure Vessels and Piping Conference, American Society of Mechanical Engineers, 2004, pp. 197-205.

[13] J. Xu, A. Askari, O. Weckner, S. Silling, Peridynamic analysis of impact damage in composite laminates, Journal of Aerospace Engineering, 21(3) (2008) 187-194.

[14] S.R. Kazemi, Plastic deformation due to high-velocity impact using ordinary state-based peridynamic theory, International Journal of Impact Engineering, 137 (2020) 103470.

[15] F. Bobaru, Y.D. Ha, W. Hu, Damage progression from impact in layered glass modeled with peridynamics, Central European Journal of Engineering, 2(4) (2012) 551-561.

[16] E. Oterkus, I. Guven, E. Madenci, Impact damage assessment by using peridynamic theory, Central European Journal of Engineering, 2(4) (2012) 523-531.

[17] N. Liu, D. Liu, W. Zhou, Peridynamic modelling of impact damage in three-point bending beam with offset notch, Applied Mathematics and Mechanics, 38(1) (2017) 99-110.

[18] B. Chen, N. Liu, G. Yang, The application of peridynamics in predicting beam vibration and impact damage, Journal of Vibroengineering, 17(5) (2015).

[19] J. Lee, W. Liu, J.-W. Hong, Impact fracture analysis enhanced by contact of peridynamic and finite element formulations, International Journal of Impact Engineering, 87 (2016) 108-119.

[20] S.A. Silling, M.L. Parks, J.R. Kamm, O. Weckner, M. Rassaian, Modeling shockwaves and impact phenomena with Eulerian peridynamics, International Journal of Impact Engineering, 107 (2017) 47-57.

[21] C. Sun, Z. Huang, Peridynamic simulation to impacting damage in composite laminate, Composite Structures, 138 (2016) 335-341.

[22] G. Zhang, G.A. Gazonas, F. Bobaru, Supershear damage propagation and sub-Rayleigh crack growth from edge-on impact: A peridynamic analysis, International Journal of Impact Engineering, 113 (2018) 73-87.

[23] Y. Song, H. Yu, Z. Kang, Numerical study on ice fragmentation by impact based on non-ordinary state-

based peridynamics, Journal of Micromechanics and Molecular Physics, (2018).

[24] F. Baber, V. Ranatunga, I. Guven, Peridynamic modeling of low-velocity impact damage in laminated composites reinforced with z-pins, Journal of Composite Materials, (2018) 0021998318774100.

[25] W. Zhou, D. Liu, Analyzing impact induced delamination in laminated composite materials with peridynamic modeling, in: 2018 AIAA/ASCE/AHS/ASC Structures, Structural Dynamics, and Materials Conference, 2018, pp. 1219.

[26] J. Zheng, F. Shen, X. Gu, Q. Zhang, Simulating failure behavior of reinforced concrete T-beam under impact loading by using peridynamics, International Journal of Impact Engineering, 165 (2022) 104231.

[27] L. Wu, D. Huang, Energy dissipation study in impact: From elastic and elastoplastic analysis in peridynamics, International Journal of Solids and Structures, 234 (2022) 111279.

[28] Y. Jafaraghaei, T. Yu, T.Q. Bui, Peridynamics simulation of impact failure in glass plates, Theoretical and Applied Fracture Mechanics, 121 (2022) 103424.

[29] M. Sun, L. Liu, H. Mei, X. Lai, X. Liu, J. Zhang, A Bond-Based Peridynamic Model with Matrix Plasticity for Impact Damage Analysis of Composite Materials, Materials, 16(7) (2023) 2884.

[30] W. Liu, J.W. Hong, Discretized peridynamics for brittle and ductile solids, International Journal for Numerical Methods in Engineering, 89(8) (2012) 1028-1046.

[31] E. Madenci, E. Oterkus, Peridynamic theory and its applications, Springer, 2014.

[32] K.M. Kpenyigba, T. Jankowiak, A. Rusinek, R. Pesci, Influence of projectile shape on dynamic behavior of steel sheet subjected to impact and perforation, Thin-Walled Structures, 65 (2013) 93-104.

[33] A. Rusinek, J.A. Rodríguez-Martínez, R. Zaera, J.R. Klepaczko, A. Arias, C. Sauvelet, Experimental and numerical study on the perforation process of mild steel sheets subjected to perpendicular impact by hemispherical projectiles, International Journal of Impact Engineering, 36(4) (2009) 565-587.

HOW TO CITE THIS ARTICLE

S.R. Kazemi, M. Shakouri, Perforation study of steel sheet under high velocity impact using Peridynamic theory, AUT J. Mech Eng., 7(2) (2023) 175-184.

DOI: 10.22060/ajme.2023.21808.6046